Electron-impact ionization of Be^+

R. Aaron Falk and Gordon H. Dunn*
Joint Institute for Laboratory Astrophysics, National Bureau of Standards and University of Colorado, Boulder, Colorado 80309

(Received 27 April 1981; revised manuscript received 19 July 1982)

The electron-impact ionization cross section for Be^+ has been measured from threshold to 1600 eV with an absolute uncertainty of 8%. The cross section has a peak value of 46.5×10^{-18} cm^2 at an energy of $\sim$50 eV, and structure ascribed to the excitation autoionization of the $1s2s2p$ state at 118.5 eV is observed. Calculations using the semiempirical formula of Lotz for direct ionization and the semiempirical effective Gaunt-factor formula for excitation autoionization give summed cross-section values which agree well with the experiment over the entire energy range. Comparisons are also made with other calculations and cross sections in the literature.

I. INTRODUCTION

Electron-impact ionization of atoms is a topic which has had the attention of researchers for more than 70 years.[1] Ionization cross sections are essential data in the modeling and understanding of hot plasmas such as those encountered in fusion research and astrophysical bodies. Despite the practical need and the long period of study, much is lacking, both in terms of our having data for a given species or ionization stage and in terms of being able to predict or theoretically derive needed data. Development of theory has been slowed by the inherent difficulty of the three (many)-body problem and by the fact that a number of different mechanisms often contributes to the total ionization cross section. Thus in addition to direct knock-on ionization of an outer-shell electron, there are the mechanisms of excitation autoionization (excitation of an inner-shell electron followed by autoionization), inner-shell ionization which is often followed by further ionization by the Auger process, and inner-shell resonant-excitation-double autoionization. These latter mechanisms can have multiple stabilization paths.

Most theoretical efforts have dealt with the direct process for ionization of either outer-shell or inner-shell electrons. This paper is not a review of the topic, and we therefore refer the reader elsewhere for adequate references and exposition. Suffice it to say that starting with the 1912 classical theory of Thomson,[2] a number of classical and semiclassical theories have evolved.[3–5] Because of the need to have data for other fields, a variety of empirical formulas[6] have come into wide application with that of Lotz[7–10] seemingly receiving widest use. Again with an eye to ready applicability, scaling formulas based on the Born[11] and Coulomb-Born[12–17] approximations have been developed. There exists only a small number of detailed specific calculations for selected isoelectronic sequences using quantum theory and modern computing methods. However, more has been done in recent times, and there are calculations for the Li isoelectronic sequence[18,19] of which Be^+ is a member.

Experimentally,[1] measurements were made on the common gases in the 1930's, and these have been substantially verified in later work. It was shown by the work of Dolder, Harrison, and Thoneman[20] on He^+ in 1961 that measurements of cross sections for electron-impact ionization of ions using crossed beams of electrons and ions can give high accuracy—perhaps better than that on neutrals. By now, cross sections have been measured for a number of ions,[21–23] and recently it has been possible to do experiments with beams of multiply charged ions[22,23] thus making it practical to examine the ionization process along an isoelectronic sequence.

Systematic studies, such as those along an isoelectronic sequence and of groupings of classes of atoms or ions, are desirable to aid the continuing effort to develop theory and predictor formulas. Such is the nature of the work presented here. By reporting cross sections for ionization of Be^+, we make more complete the study of the Li isoelectronic sequence, adding to the data of Crandal *et al.*[24–26] on C^{3+}, N^{4+}, and O^{5+} and to the data of several authors[27–29] on Li. Also, these data help complete a grouping of cross sections for ions of the alkaline earths, adding to the work of Dolder *et al.*[30–33] and of Feeney *et al.*[34]

In making comparisons with these groupings later, it will be important to pay specific attention to the scaling of the cross sections for the direct pro-

cess and of the cross-section contributions from excitation autoionization.

II. EXPERIMENTAL PROCEDURE

A. Apparatus and technique

Generally, the experiment utilized the crossed-charged-beams technique.[21] A schematic view of the apparatus is shown in Fig. 1. A well-collimated beam of Be^+ ions is crossed with a magnetically confined electron beam. A parallel-plate electrostatic analyzer spatially separates the primary and product ions, and they are collected and the currents measured using separate collectors.

The cross section is deduced from experimental parameters using the relationship[21]

$$\sigma=\frac{\mathscr{R}e^2}{I_eI_i}\frac{v_iv_e}{(v_i^2+v_e^2)^{1/2}}\frac{\mathscr{F}}{D_{2+}}\ , \tag{1}$$

where I_i, I_e, v_e, and v_i are the currents and velocities, respectively, of electrons and ions, D_{2+} is the probability that a doubly charged ion produced by electron impact will be detected, and $\mathscr{R}$ is the measured counting rate of doubly charged ions. The form factor $\mathscr{F}$ takes account of the spatial overlap of the two beams, and is given by

$$\mathscr{F}=\frac{\int R(z)\,dz\int G(z)\,dz}{\int R(z)G(z)\,dz}\ , \tag{2}$$

where $R(z)$ and $G(z)$ are the relative vertical distributions of the electron- and ion-beam current densities.

The electron gun used was one for which the characteristics have been studied in detail, and the gun properties have been published.[35] The gun has been used in the crossed-beams configuration for numerous experiments previously reported. The electron beam, produced from an oxide-coated nickel cathode, is magnetically confined by a 0.02-T longitudinal field, and is collected in a gold-blacked collector equipped with a honeycomb surface to minimize reflections. The collector is positively

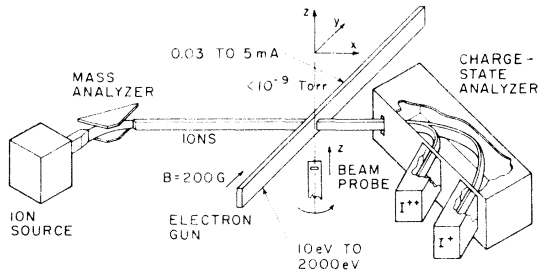

FIG. 1. Schematic of experiment.

biased to prevent escape of secondary electrons. Secondary electrons were thus no problem; however, at high energies reflected electrons necessitated an energy-dependent correction ranging up to 10% and also led to higher uncertainties above 400 eV.

The electron energy in eV is given by

$$E_e=V_c-\phi-\frac{S}{\sqrt{V_e}}I_e+\frac{A}{\sqrt{V_i}}S_iI_i\ , \tag{3}$$

and the energy spread is given by

$$\Delta E_e=\Delta V_{\rm th}+\frac{S'}{\sqrt{V_e}}I_e\ . \tag{4}$$

Here E_e and ΔE_e are the true electron laboratory energy and energy spread, V_c is the applied cathode potential, ϕ is a constant accounting for contact potential, $S=0.071$, $S_i=3.0$, and $S'=0.017$ are constants (units $eV^{3/2}\mu A^{-1}$) depending on beam and electrode geometry which account for space-charge effects, A is the atomic number of the ions under investigation, V_i the ion energy, and $\Delta V_{\rm th}=0.22$ eV is the energy width (primarily thermal) exclusive of space-charge effects. The effect of electron spiraling in the beam has been studied[35] and corrected for. The beam is 2 mm wide by 6 mm high, and the energy is changed by changing V_c.

The Be^+ ions were produced in a simple, commerical, hot-filament, discharge-ion source.[36] Chips of Be metal were placed in the discharge crucible and a discharge struck with CCl_4. Resultant reactions with the Be provided a source of more volatile $BeCl_4$, which was subsequently ionized in the discharge. The ions were extracted through a 0.5-mm hole in the molybdenum anode, mass analyzed, and transported via focusing and collimating optics to the interaction region where the beam was 2 mm wide by 2 mm high. The laboratory ion energy was 2300 eV. The energy spread from the ion source has been reported[36] to be less than 1 eV, but the spread was not specifically measured in these experiments. However, the spread was limited by the mass analyzer to about 12 eV, so that the uncertainty introduced in σ through the uncertainty in v_i in Eq. (1) is about 0.3%. The spread in ion energies has a totally negligible effect on the spread of interaction energy. The total electron-ion interaction energy is given by

$$E=\mu(E_i/m_i+E_e/m_e)\ ,$$

where m_i and m_e are the respective masses, and μ is the reduced mass. This reduces to give approximately

$$E\approx E_e+m_e/m_i(E_i-E_e)$$

and is basically just the electron energy "corrected"

by an energy the order of 0.1 eV.

The analyzer is the one used in this laboratory[37] for electron-impact dissociation of H_2^+ and has been described earlier. It is of the 45° parallel-plate variety similar to that described by Yarnold and Bolton[38] and first used by Lineberger *et al.*[39] for crossed-charged-beams work. Two modifications[40] were incorporated into the analyzer: (1) the product ion Faraday cup was replaced with a large area electron multiplier to permit particle counting, and (2) a set of vertical deflection plates was added at the entrance slit to correct for the ion-beam deflection by the 0.02-T magnetic field of the electron gun. The primary beam Faraday cup was constructed to minimize reflections, and a biased guard ring before the cup precluded the escape of secondary electrons. Tests showed that neither reflections nor secondary electrons led to uncertainties in current measurement greater than 0.5%, but uncertainties from these sources are included in the budget of uncertainties discussed later.

The beam profiles $R(z)$ and $G(z)$ appearing in Eq. (2) were measured by observing the currents transmitted through a 0.25-mm slit as the slit was scanned through the relevant range of z. The probe could be scanned through one beam with the plane of the slit surface perpendicular to that beam, then rotated by 90° and scanned through the other beam. In this way the beam profiles were measured along the actual line of intersection. The electron beam was generally taller than the ion beam and was usually quite uniform, so that $\mathscr{T}$ in Eq. (2) was approximately equal to the height of the electron beam and varied by less than 20% over the entire energy range of the measurements.

Tests showed that the electron beam did not produce any background in the signal detector, while the ion beam produced background counts of order 2×10^4 sec^{-1} per μA ion beam. This compares to signals (e.g., at 100 eV) of 8×10^3 sec^{-1} per μA ion beam. Thus the electron beam was chopped[41] at typically 250 Hz, and gated scalers were used to separately record "signal plus background" and "background."

B. Data collection and absolute calibration

Relative measurements of the cross section were made using the electron multiplier at the I^{2+} collector and counting individual pulses. An energy range was selected over which the form factor [Eq. (2)] did not change by more than 3% (such changes were found to be monotonic with energy); the interval was divided into as many as 30 distinct energies. Form factors were then measured for energies at the ends and middle of the interval, measurements taken at ten energies spanning the interval, form factors taken again, measurements at another ten energies spanning the interval, and so on until the statistical precision was adequate. In each set of ten energies and in each set of form factors, measurements were included at a reference energy (100 eV), so that repetitive sets could be combined and sets at different energies put on a common plot. During all the measurements, values at the reference energy fluctuated over a range typically less than ±5% of the value.

The absolute cross section was determined by measuring the quantities in Eq. (1) as in the relative measurements, but the current through the I^{2+} slit was measured using a calibrated vibrating reed electrometer, so that the quantity $I^{2+}/2e$ replaces $\mathscr{R}$ in Eq. (1). Precautions were taken to ensure that use of the multiplier as a Faraday cup did not suffer from common problems such as escape of secondary electrons, reflection of ions, etc. A beam of I^{2+} ions deflected alternately to the I^+ Faraday cup and to the I^{2+} collector was measured to be the same within 0.2%. Thus for these absolute measurements D_{2+} in Eq. (1) was unity. The absolute cross section was measured only at 400 eV, and the relative measurements were made absolute by tying to this point, which was measured more than 50 times to establish sufficient precision.

C. Consistency checks and uncertainties

The crossed-charged-beams technique lends itself to detailed systematic checks and diagnostics, and such checks have been reported in detail from the laboratories of Dolder *et al.*,[21,42] Harrison *et al.*,[43] Hooper *et al.*,[34,39,44] from this laboratory,[45] and others. The pitfalls and difficulties such as false signals from space charge or pressure change, beam collection and measurement, and ion-beam metastable

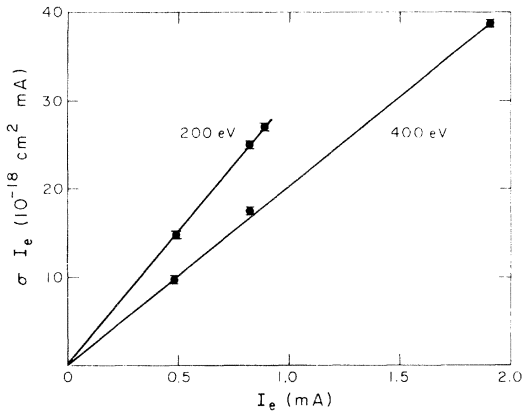

FIG. 2. Signal, normalized for ion current and form factor, vs electron current [see Eq. (1)].

TABLE I. Examples of raw data at 92.4 eV interaction energy. Scalers give counts for 30-sec integrations. Currents are also integrated values (averages over the 30 sec). Scaler 1 collects backgrounds, scalar 2 both background and signal. There is a 0.96 duty cycle factor due to certain time delays in the chopping scheme. The examples are shown to cover a range of ion currents.

Scaler 1	Scaler 2	I_e (μA)	I_i (μA)	$\mathcal{F}$ (cm)	σ (10^{-18} cm^2)
9276	13372	131.39	0.0338	0.425	38.19
23624	29787	128.11	0.0572	0.482	38.80
22285	28698	128.93	0.0610	0.490	38.19
27754	38478	139.61	0.0844	0.440	39.02
33396	45311	129.75	0.1056	0.451	38.23

contamination have been identified and discussed in the above papers. The present work has been set up to avoid or minimize the problems, and the apparatus has been thoroughly checked and uncertainties assessed. These checks result in plots, an example of which is shown in Fig. 2, which demonstrate proper dependence or independence of the cross section on experimental parameters. The plot in Fig. 2 shows the linearity of signal with I_e and demonstrates that the measured cross section is independent of space-charge effects for the current range used. Table I shows examples of raw data at 92.4 eV energy for a range of ion currents. These data represent single 30-sec "integrations" of measured parameters. A measurement normally consisted of several such integrations—until statistical precision was adequate. These data, when plotted as in Fig. 2— or in other ways as it may please the reader— show linear dependence of signal (or independence of cross section) on ion current.

The budget of uncertainties resulting from tests and evaluation of the experiment is given in Table II. Uncertainties are estimated to be at the 1σ level (68% confidence level).

TABLE II. Uncertainties in absolute value (1σ equivalent).

Source	Uncertainty (%)
Standard deviation of mean of measurement for absolute point	7.3
Transmission of analyzer	0.75
False "signal"[a]	1
Incident electron current	0.5
Incident ion current	0.5
Form factor	2.2
Uncertainty in electron and ion energies	0.3
Calibration of vibrating reed electrometer	1
Quadrature sum	7.8

[a]False "signals" can arise from such sources as space-charge modulation of background stripped ions or modulation of background gas density.

III. RESULTS AND DISCUSSION

A plot of Be^+ ionization cross section versus energy is shown by the open circles in Fig. 3. The bars shown represent one standard deviation of the mean, are typical for that energy region, and represent the statistical uncertainty of the points as determined by the run-to-run reproducibility of the data. The absolute total uncertainty as determined at the 400-eV benchmark point is about 7%. Table III lists the cross-section values and statistical uncertainties.

Table IV shows the comparison of our data to the

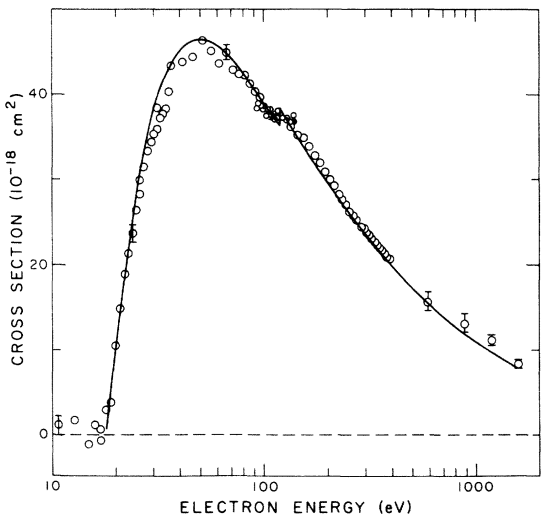

FIG. 3. Cross section vs energy for electron-impact ionization of Be^+. Open circles are experimental data, and bars represent one standard deviation of the mean and are typical for a given energy region. Line is from Eq. (5). Uncertainty in the absolute value is about ±7% (see Table I).

TABLE III. Absolute cross sections for electron-impact ionization of Be^+.

Energy (eV)	$\sigma\pm\Delta\sigma$ (10^{-18} cm^2)		Energy (eV)	$\sigma\pm\Delta\sigma$ (10^{-18} cm^2)		Energy (eV)	$\sigma\pm\Delta\sigma$ (10^{-18} cm^2)	
18.8	3.7	±0.7	91.4	40.3	±0.4	164.2	33.8	±0.5
19.9	10.5	±1.2	92.4	38.7	±0.4	174.3	32.8	±0.5
20.8	14.9	±1.2	93.4	39.0	±0.5	184.4	32.0	±0.3
20.9	15.0	±0.7	94.4	39.0	±0.5	194.8	30.9	±0.4
21.9	18.7	±0.9	96.2	38.6	±0.3	205.0	30.0	±0.3
22.9	21.3	±1.0	98.2	38.2	±0.5	215.0	29.2	±0.4
23.9	23.6	±1.1	100.2	38.5	±0.4	225.0	28.0	±0.3
24.9	26.2	±1.3	102.2	37.4	±0.5	235.0	27.6	±0.4
25.9	29.1	±1.0	104.2	38.2	±0.7	245.0	27.0	±0.3
26.9	31.4	±0.8	106.6	38.3	±0.6	255.0	26.2	±0.4
27.9	33.3	±0.6	108.6	37.5	±0.4	265.0	25.7	±0.4
29.0	34.3	±0.9	110.5	37.3	±0.4	275.0	25.2	±0.4
30.0	35.4	±0.6	112.5	36.7	±0.4	286.0	24.5	±0.5
31.0	37.4	±0.6	114.5	37.1	±0.5	296.0	24.4	±0.5
32.0	32.2	±1.0	116.5	36.2	±0.6	306.0	23.7	±0.6
33.0	33.0	±0.8	118.4	37.6	±0.6	316.0	23.5	±0.6
34.1	38.2	±0.8	120.4	37.5	±0.5	326.0	23.1	±0.6
35.1	40.1	±0.9	122.4	37.1	±0.6	336.0	22.6	±0.6
36.0	42.9	±1.0	124.7	37.7	±0.5	346.0	22.2	±0.7
41.1	43.7	±0.9	126.5	36.9	±0.6	356.0	22.0	±0.7
46.2	44.4	±0.9	128.5	37.0	±0.5	366.0	21.7	±0.7
51.2	46.3	±0.8	130.4	36.7	±0.5	377.0	22.4	±0.7
56.2	45.0	±0.6	132.4	36.5	±0.4	387.0	20.9	±0.7
61.3	43.5	±0.6	133.8	36.2	±0.6	397.0	20.7	±0.8
66.3	45.0	±0.4	134.4	35.8	±0.4	586.0	15.7	±1.2
71.3	42.9	±0.5	136.6	36.5	±0.4	890.0	13.1	±1.2
76.3	42.3	±0.5	138.2	35.7	±0.5	1191.0	11.1	±0.6
81.4	42.2	±0.4	143.9	35.1	±0.7	1592.0	8.4	±0.3
86.4	41.3	±0.5	154.0	34.8	±0.4			

low-energy quantum calculations of Younger,[18] in which use was made of several approximations as shown in the caption. The CBE calculation shows good agreement with the experimental data. The other approximations give results too small at the low energies where calculations were made.

Referring again to Fig. 3, we see that near 118 eV a distinct change of slope can be seen in the data. This is shown in more detail in Fig. 4. The onset of inner-shell ionization does not occur until 140 eV and is estimated to be too small ($<1\%$) to account for this observation. The 118-eV feature is identified as being due to the excitation autoionization of the $1s2s2p$ state of Be^+. Griffin[46] has calculated the energy of the $1s2s2p$ state to be 118.5 eV with an optical oscillator strength (f value) of 0.62.

The solid curve in Figs. 3 and 4 is seen to represent the data very well. The curve was ob-

TABLE IV. Be^+ scaled electron-impact ionization cross section UI^2Q, where $U=E/I$, E is electron energy, and $I=1.339$ Ry is the threshold ionization energy. Units are $\pi a_0^2(\text{Ry})^2$. Theoretical values owing to Younger (Ref. 20).

U	DWE[a]	DWT[a]	CBE[a]	CBT[a]	PWB[a]	Experimental Data
1.125	0.269	0.237	0.310	0.234	0.145	0.31±0.02
1.25	0.493	0.467	0.564	0.462	0.334	0.55±0.04
1.50	0.866	0.903	0.973	0.891	0.752	0.96±0.07
2.25	1.67	1.94	1.80	1.92	1.79	1.98±0.14

[a]DWE, distorted wave with exchange; DWT, distorted wave truncated; CBE, Coulomb-Born with exchange; CBT, Coulomb-Born truncated; PWB, plane-wave Born.

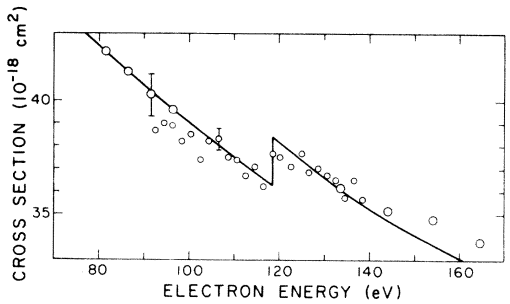

FIG. 4. Detail of Be^+ ionization cross section near the $1s2s2p$ autoionizing state. See Fig. 3.

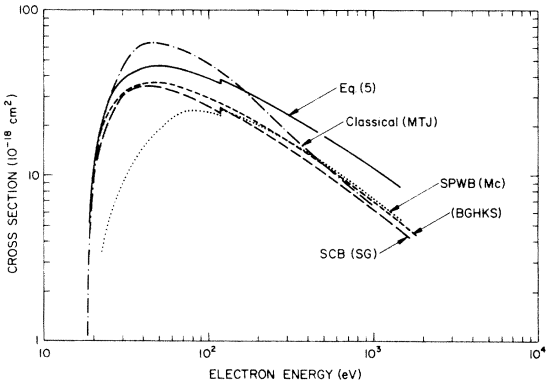

FIG. 5. Log-log plot of ionization cross section for Be^+ vs electron energy. Solid curve is the same as in Fig. 3 [computed from Eq. (5)] and is taken to closely represent the data. The short-dashed curve is the "recommended" cross section curve of Bell *et al.* (Ref. 50); long-dashed curve is from the SCB formulas of Sampson and Golden (Ref. 17); dotted curve is from the SPWB formulas of McGuire (Ref. 11); dot-dashed curve is from the modified classical binary-encounter model of Thomas and Garcia (Ref. 52) as calculated by Mathur *et al.* (Ref. 51).

tained from the representation

$$\sigma = 0.95\sigma_L + \sigma_{\bar{g}} \ . \tag{5}$$

Here σ_L is the cross section calculated using the Lotz[7–10] predictor formula

$$\sigma_L = \sum_i \frac{a_i q_i}{EI_i} \ln(E/I_i)\{1 - b_i \exp[-c_i(E/I_i - 1)]\} \ , \tag{6}$$

where a_i, b_i, and c_i are fitting constants given by Lotz, I_i is the ionization energy of electrons in the ith subshell, q_i is the number of electrons in the ith subshell, and E is the electron energy. For Be^+, $a_1 = 4.4\times10^{-14}$, $a_2 = 4\times10^{-14}$, $b_1 = 0$, $b_2 = 0.4$, $c_1 = 0$, $c_2 = 0.6$, $q_1 = 1$, $q_2 = 2$, $I_1 = 18.2$ eV, and $I_2 = 140$ eV. The 0.95 scaling factor multiplying σ_L is chosen simply to obtain a fit to the data. The excitation autoionization contribution to σ is taken in Eq. (5) to be simply the cross section for excitation of the $1s2s2p$ state as represented by the effective Gaunt-factor predictor formula,[47–49]

$$\sigma_{\bar{g}} = \frac{8\pi}{\sqrt{3}} \frac{R^2}{\Delta^2} f \frac{\bar{g}(X)}{X} \pi a_0^2 \ . \tag{7}$$

Here $X = E/\Delta$ is the energy in units of the threshold energy Δ, f is the optical oscillator strength, R is the Rydberg energy, a_0 is the radius of the first Bohr orbit, and $\bar{g}(X)$ is a function[49] called the effective Gaunt factor. The particularly good agreement between the measured cross sections and the "predicted" cross section [Eq. (5)] is possibly fortuitous given the usual uncertainties associated with the use of Eqs. (6) and (7).

Bell *et al.*[50] have recently compiled a set of "recommended" cross sections for light atoms and ions. They fit all cross sections to a formula with several fitting parameters. For Be^+ they chose to fit to Younger's DWE results with the consequence that their "recommended" cross section function for Be^+ ranges from 15% low at low energies to 23% low at the peak and ~60% low at high energies, when compared with the measurements of this experiment. Their recommended cross-section function is illustrated in Fig. 5 as the short-dashed curve.

Shown as the solid curve in Fig. 5 is the same curve as in Fig. 4 [i.e., Eq. (5)], which is taken for these comparisons as representing the experimental data fairly well. The dotted curve is from the scaled plane-wave Born (SPWB) method of McGuire.[11] The long-dashed curve represents the prediction of the scaled Coulomb-Born (SCB) method of Sampson and Golden.[17] To both of these latter predictions, we have added $\sigma_{\bar{g}}$ from Eq. (7). The dot-dashed curve is from the paper by Mathur *et al.*[51] who used the modified classical binary-encounter model of Thomas and Garcia.[52]

Excitation autoionization associated with the $1s2s2p$ state is also manifest in the cross sections for other lithiumlike ions on which measurements have been made,[24–26] C^{3+}, N^{4+}, and O^{5+}. Figure 6 shows the trend with charge state of the relative importance of the direct and indirect processes. Here the ratio of the cross section at the second peak associated with excitation autoionization to the cross section at the first peak associated with direct ionization is plotted versus initial ionic charge $(Z-3)$. The points are experimental from the sources cited. The chain curve in the figure is that calculated by Sampson and Golden.[17] Clearly, the indirect process becomes relatively more important with increasing

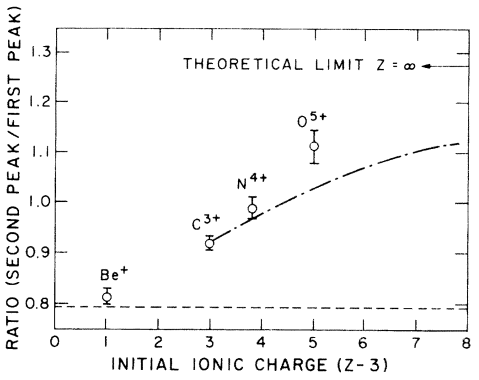

FIG. 6. Plot of the ratio of the cross-section value at the excitation autoionization peak to the value at the peak for the direct process. C^{3+}, N^{4+}, and O^{5+} data due to Crandall *et al.* (Refs. 24–26). The theoretical curve (dash-dot) owing to Sampson and Golden (Ref. 17); the infinite Z limit neglects the increasing role of radiative decay as Z is increased. Bars are one standard deviation relative uncertainty.

charge state. The present work on Be^+ fits the theoretical and experimental trends well, and the single point associated with O^{5+} signals significant disagreement with the theory. It appears that investigation of higher charge states and/or reinvestigation of O^{5+} may be worthwhile to firmly establish this.

A comparison of the cross sections for ionization of all the singly ionized alkaline-earth metals[30–34] (except radium) is shown in Fig. 7. Strong excitation-autoionization contributions are seen at low energies in Ca^+, Sr^+, and Ba^+ associated with *np-nd* transitions. Analogous $\Delta n=0$ transitions are

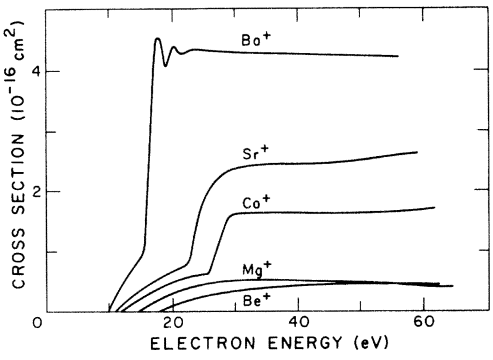

FIG. 7. Electron-impact ionization cross sections for the singly ionized alkaline-earth metals; Be^+ from this work, others from Refs. 30–34.

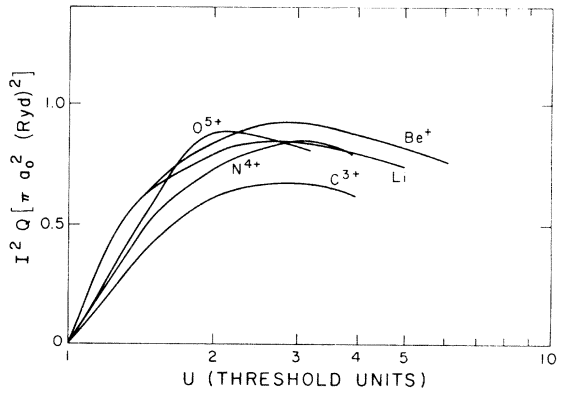

FIG. 8. Scaled cross sections for the lithiumlike isoelectronic sequence. $U=E/I$ where E is the electron energy and I is the threshold ionization energy. Be^+ from this work; C^{3+}, N^{4+}, and O^{5+} from Refs. 24–26; Li from Ref. 28.

not possible in Mg^+ and Be^+, but we have seen in this paper a 5% contribution to the Be^+ cross section from the $1s^22s$-$1s2s2p$ transition ($\Delta n=1$). Recent work in this laboratory[53] on Mg^+ shows contributions from similar $\Delta n=1$ transitions of about 10%. More detailed data for the other alkaline-earth metal ions at higher energies should show analogous contributions.

Figure 8 shows the experimentally measured cross sections for the lithiumlike isoelectronic sequence in units of $\pi a_0^2 I^2$, where a_0 is the Bohr radius and I is the threshold energy in rydbergs. In the figure $U=E/I$, where E is the electron-impact energy. The cross sections are plotted only to the energy onset for excitation autoionization. Simple classical theory[2] indicates that in these units the cross sections can be represented by a single universal function. With the exception of C^{3+} a universal function could indeed be adopted which would give values accurate to $\sim 10\%$. The ion O^{5+} seems anomalous in that the peak appears at a U of ~ 2 as compared to ~ 2.8 for the other ions. One notes that a focusing action is expected[54] from the Coulomb field, and some pulling in of the peak for high charge states is an expected result. The Be^+ results are from this work, the C^{3+}, N^{4+}, and O^{5+} from Refs. 24–26, and the Li data are from Ref. 28.

Note added in proof. Bell *et al.* have informed us that versions of the manuscript being submitted for publication have been changed to recommend Be^+ cross sections which follow the data of this paper.

ACKNOWLEDGMENTS

We are grateful to Dr. D. C. Griffin for his calculation of the position of the $1s2s2p$ state. This work was supported in part by the Office of Magnetic Fusion Energy, U.S. Department of Energy.

*Staff members: Quantum Physics Division, National Bureau of Standards.

[1]For reviews, see L. J. Kieffer and G. H. Dunn, Rev. Mod. Phys. 38, 1 (1966); also see H. S. W. Massey, E. H. S. Burhop, and H. B. Gilbody, *Electronic and Ionic Impact Phenomena, Vol. I* (Oxford University Press, London, 1969), Chap. 3, p. 97.

[2]J. J. Thomson, Philos. Mag. 23, 449 (1912).

[3]M. Gryzinski, Phys. Rev. 115, 374 (1959); 138, A305 (1965); 138, A322 (1965); 138, A336 (1965).

[4]B. K. Thomas and J. D. Garcia, Phys. Rev. 179, 94 (1969).

[5]A. Burgess, in *Atomic Collision Processes,* edited by M. R. C. McDowell (North-Holland, Amsterdam, 1964), p. 237; Atomic Energy Research Establishment Report No. 4818, 1964 (unpublished), p. 63; A. Burgess and I. C. Percival, Adv. At. Mol. Phys. 4, 109 (1968).

[6]For reviews, see T. Kato, Institute of Plasma Physics, Nagoya University, Nagoya, Japan, Report No. IPPJ-AM-2 (unpublished); Y. Itikawa and T. Kato, Report No. IPPJ-AM-17 (unpublished).

[7]W. Lotz, Astrophys. J. Suppl. Ser. 14, 207 (1967).

[8]W. Lotz, Z. Phys. 216, 241 (1968).

[9]W. Lotz, Z. Phys. 220, 466 (1969).

[10]W. Lotz, Z. Phys. 206, 205 (1967).

[11]E. J. McGuire, Phys. Rev. A 16, 73 (1977).

[12]L. B. Golden and D. H. Sampson, J. Phys. B 10, 2229 (1977).

[13]D. H. Sampson and L. B. Golden, J. Phys. B 11, 541 (1978).

[14]L. B. Golden, D. H. Sampson, and K. Omidvar, J. Phys. B 11, 3235 (1978).

[15]D. L. Moores, L. B. Golden, and D. H. Sampson, J. Phys. B 13, 385 (1980).

[16]L. B. Golden and D. H. Sampson, J. Phys. B 13, 2645 (1980).

[17]D. H. Sampson and L. B. Golden, J. Phys. B 12, L785 (1979).

[18]S. M. Younger, Phys. Rev. A 22, 111 (1980).

[19]H. Jakubowicz and D. L. Moores, J. Phys. B 14, 3733 (1981).

[20]K. T. Dolder, M. F. A. Harrison, and P. C. Thonemann, Proc. R. Soc. London, Ser. A 264, 367 (1961).

[21]K. T. Dolder and B. Peart, Rep. Prog. Phys. 39, 693 (1976).

[22]G. H. Dunn, in *The Physics of Ionized Gases,* edited by M. Matic' (Boris Kidric' Institute of Nuclear Sciences, Belgrade, 1980), pp. 49–95.

[23]D. H. Crandall, Phys. Scr. 23, 153 (1981).

[24]D. H. Crandall, R. A. Phaneuf, and P. O. Taylor, Phys. Rev. A 18, 1911 (1978).

[25]D. H. Crandall, R. A. Phaneuf, and B. E. Hasselquist, and D. C. Gregory, J. Phys. B 12, L249 (1979).

[26]D. H. Crandall, R. A. Phaneuf, and D. C. Gregory, Report No. ORNL/TM-7020, Oak Ridge National Laboratory, Oak Ridge, Tennessee (unpublished).

[27]G. O. Brink, Phys. Rev. 127, 1204 (1962).

[28]I. P. Zapesochnyĭ and I. S. Aleksakhin, Zh. Eksp. Teor. Fiz. 55, 76 (1968) [Sov. Phys.—JETP 28, 41 (1969)].

[20]R. Jalin, R. Hagemann, and R. Botter, J. Chem. Phys. 59, 952 (1973).

[30]B. Peart and K. T. Dolder, J. Phys. B 8, 56 (1975).

[31]B. Peart and K. T. Dolder, J. Phys. B 1, 872 (1968).

[32]B. Peart, J. G. Stevenson, and K. T. Dolder, J. Phys. B 6, 146 (1973).

[33]O. S. Martin, B. Peart, and K. T. Dolder, J. Phys. B 1, 537 (1968).

[34]R. K. Feeney, J. W. Hooper, and M. T. Elford, Phys. Rev. A 6, 1469 (1972).

[35]P. O. Taylor, K. T. Dolder, W. E. Kauppila, and G. H. Dunn, Rev. Sci. Instrum. 45, 538 (1974).

[36]M. Menzinger and L. Wahlin, Rev. Sci. Instrum. 40, 102 (1969).

[37]G. H. Dunn and B. Van Zyl, Phys. Rev. 154, 40 (1967).

[38]G. D. Yarnold and H. C. Bolton, J. Sci. Instrum. 26, 38 (1949).

[39]W. C. Lineberger, J. W. Hooper, and E. W. McDaniel, Phys. Rev. 141, 151 (1966).

[40]W. T. Rogers, G. Stefani, R. Camilloni, G. H. Dunn, A. Msezane, and R. J. W. Henry, Phys. Rev. A 25, 737 (1982).

[41]Measurements to 400 eV were made using chopped beam techniques. Past 400 eV, dc beams were used, and though measurements presented no problems, a larger uncertainty resulted. Electronic units used in this particular experiment were built to chop only to 400 eV, and though we have other units capable of chopping to about 2 keV, they were not available during the course of these measurements.

[42]K. T. Dolder, in *Case Studies in Atomic Collision Physics,* edited by E. W. McDaniel and M. R. C. McDowell (North-Holland, Amsterdam, 1969), Vol. 1, p. 249.

[43]M. F. A. Harrison, Br. J. Appl. Phys. 17, 371 (1966); M. F. A. Harrison, in *Methods in Experimental Physics,* edited by W. L. Fite and B. Bederson (Academic, New York, 1968), Vol. 7A, pp. 95–115.

[44]J. W. Hooper, W. C. Lineberger, and F. M. Bacon, Phys. Rev. 141, 165 (1966).

[45]G. H. Dunn, in *Atomic Physics,* edited by B. Bederson, V. W. Cohen, and F. M. J. Pichanick (Plenum, New York, 1969), pp. 417–433.

[46]D. C. Griffin (private communication).

[47]A. Burgess, Mem. Soc. R. Sci. Liege Collect. 8° 4, 299 (1961).

[48]M. J. Seaton, in *Atomic and Molecular Process,* edited by D. R. Bates (Academic, New York, 1962), p. 372.

[49]H. Van Regemorter, Astrophys. J. 136, 906 (1962).

[50]K. L. Bell, H. B. Gilbody, J. G. Hughes, A. E. Kingston, and F. J. Smith (see note added). Culham Laboratory Report No. CLM-R216 (unpublished).

[51]K. C. Mathur, A. N. Tripathi, and S. K. Joshi, Astrophys. J. 165, 425 (1971).

[52]B. K. Thomas and J. D. Garcia, Phys. Rev. 179, 94 (1969).

[53]D. H. Crandall, R. A. Phaneuf, R. A. Falk, D. S. Belic, and G. H. Dunn, Phys. Rev. A 25, 143 (1982).

[54]G. Peach, J. Phys. B 4, 1670 (1971).